



EDINBURGH
INSTRUMENTS



SCAN ME

RAMAN AND BEYOND...

- + Multi-modal Confocal Microscopy
- + Raman & Photoluminescence Mapping
- + Fluorescence & Phosphorescence Lifetime Imaging (FLIM/PLIM)



MANUFACTURED
WITH PRIDE IN THE
UNITED KINGDOM

edinst.com

RESEARCH ARTICLE

Comparative performance of theoretical tools in order to quantify the effect of the electric potential on the vibrational wavenumbers and intensities of the SERS of 2-methylpyrazine adsorbed on a nanostructured silver electrode

Samuel Valdivia¹  | Daniel Aranda²  | Juan Soto¹  | Juan Carlos Otero¹  | Isabel López-Tocón¹ 

¹Andalucía Tech, Departamento de Química Física, Facultad de Ciencias, Universidad de Málaga, Málaga, Spain

²Instituto de Ciencia Molecular (ICMol), Universidad de Valencia, Paterna, Spain

Correspondence

Isabel López-Tocón, Andalucía Tech, Departamento de Química Física, Facultad de Ciencias, Universidad de Málaga, Málaga, Spain.
Email: tocon@uma.es

Funding information

Consejería de Conocimiento, Investigación y Universidad, Junta de Andalucía, Grant/Award Numbers: P18-RT-4592, UMA18-FEDERJA-049; Generalitat Valenciana, Grant/Award Number: APOSTD/2021/025; Junta de Andalucía/FEDER; University of Málaga and Generalitat Valenciana/European Social Fund

Abstract

The effect of the electrode potential in surface-enhanced Raman scattering (SERS) intensities and wavenumbers of 2-methylpyrazine (2MP) was analyzed on the basis of a resonant charge transfer (CT) mechanism by using a simple theoretical model in which the metallic surface and its charge density were simulated by atomic silver clusters of different size (n) and charge (q), $[\text{Ag}_n]^q$. Two linear silver atoms ($n = 2$) with zero charge ($q = 0$) and three linear silver atoms ($n = 3$) with positive and negative charges ($q = \pm 1$) linked to the two nonequivalent aromatic nitrogen atoms in 2MP were taken into account. The wavenumber shifts of the most intense bands and the SERS-CT spectra of these two types of metal-adsorbate supermolecule, $[\text{Ag}_n\text{-N1}]^q$ and $[\text{Ag}_n\text{-N4}]^q$, were calculated by using a time-dependent density functional theory (TD-DFT) method and the independent mode displaced harmonic oscillator (IMDHO) approximation. A comparison of the effect of different levels of calculation, *ab initio*/DFT, on the predictions from the two theoretical models (isolated adsorbate/supermolecule) is also performed. Only DFT theoretical results of the metal-adsorbate supermolecule allow to explain the main role of the pair of bands assigned to totally symmetric ring-stretching 8a,b modes. The 8a vibration is the strongest band at any electrode potential, whereas the 8b mode reaches a maximum enhancement at -0.50 V and then decreases at -0.75 V. This model of a charged metal-adsorbate interface allows for detecting the presence of a CT mechanism in a SERS record.

Samuel Valdivia and Daniel Aranda contributed equally.

This is an open access article under the terms of the [Creative Commons Attribution-NonCommercial-NoDerivs](https://creativecommons.org/licenses/by-nc-nd/4.0/) License, which permits use and distribution in any medium, provided the original work is properly cited, the use is non-commercial and no modifications or adaptations are made.

© 2022 The Authors. *Journal of Raman Spectroscopy* published by John Wiley & Sons Ltd.

KEYWORDS

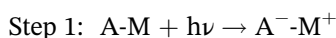
2-methylpyrazine, charge transfer mechanism, nanostructured electrode, SERS spectroscopy, TD-DFT calculation

1 | INTRODUCTION

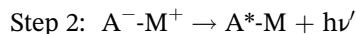
The knowledge of the surface-enhanced Raman scattering (SERS) phenomenon^[1,2] is still a challenge. Questions like which mechanism mainly contributes to the SERS enhancement,^[3–5] what selection rules can be applied to explain the enhanced bands,^[6–8] or how some experimental parameters, that is, the excitation wavelength and the potential electrode, affect a SERS record in electrochemical experiments^[4,9] are still open.

In most works of SERS concerning aromatic molecules, the changes in the relative intensities are analyzed by considering the selection rules of the electromagnetic (EM) enhancement mechanism^[10,11] because it is considered the major contributor to the global SERS enhancement. These selection rules, which are similar to those of surface IR spectroscopy and labeled as propensity rules, yield effortless information about the molecular adsorption interaction and the orientation of the adsorbate with respect to metal surface. Nowadays, the understanding of the charge transfer (CT) enhancement mechanism^[12,13] in a SERS record is acquiring more importance because it is able to explain the differentiated behavior of the enhanced SERS bands in structurally similar benzene-like molecules^[14–16] and also, it seems to be related to the blinking effect in single-molecule SERS events.^[17] Nevertheless, the analysis of SERS spectra from the CT mechanism point of view is a difficult task because SERS-CT-enhanced vibrations depend on the particular properties of the electronic states involved in the photoinduced resonance CT process of the metal-adsorbate system. For this reason, there is no universal selection rule for the CT mechanism unlike what occurs for the EM one, in which the so-called “propensity rules” similar to those of surface IR spectroscopy are established.^[1]

Our research group has developed a systematic procedure^[16] in order to detect and estimate the CT contribution to a SERS record assuming that it is similar to a photoinduced resonance Raman (RR)^[18] process with two steps. The laser photon ($h\nu$) produces the resonant transfer of one electron from the Fermi level of the metal (M) to vacant orbitals (LUMO or other up in energy) of the adsorbate (A) yielding the excited CT state ($A^- \cdot M^+$):



When the electron comes back to the metal in Step 2, a Raman photon is emitted if the molecule remains vibrationally excited (A^*).



According to this process, the activity of the CT-enhanced fundamentals can be due to the first term that mainly contributes to the RR intensities, A-term, also called Franck–Condon factor,^[6] which is related to the geometrical displacement between the two equilibrium structures of the resonant electronic states. Thus, the resonant process considering the whole metal-adsorbate system is given between the ground electronic state, S_0 state, and that excited with CT characteristics called CT_0 state, which is analog to a doublet state of the radical anion, from an adsorbate point of view, being called D_0 state.^[14]

The resonant SERS-CT condition depends not only on the excitation wavelength, like any resonance process but also on the electrode potential, which tunes the energy of the Fermi level of the metal yielding a huge energy gain in electrochemical SERS experiments.^[19] Therefore, the electrode potential plays a key role in the SERS-CT effect, and the analysis of the electrochemical SERS experiments under applied voltage allows getting insight into the nature of the CT mechanism and shedding light on the CT excited electronic states.

From a theoretical point of view, a model of the metal-adsorbate surface complex must be established to elucidate its electronic structure by using quantum mechanical calculations based on density functional theory (DFT).^[20] Our group proposes that the macroscopic electrode potential can be simulated by several linear metallic clusters with different charge densities ($q_{\text{eff}} = q/n$) changing the number of silver atoms (n) and charges (q), $[Ag_n]^q$. This simple model reproduces theoretically the amount and the sign of the excess of charge on the metallic surface, and it is able to explain the different behavior of the relative SERS-CT intensities of benzene-like molecules such as pyridine,^[20] pyridazine,^[14] or 3-methylpyridine^[8] and the voltage dependence on the SERS wavenumbers of cyanide^[9] or 4-cyanobenzoate^[21] ions adsorbed on a charged nanostructured silver electrode.

In this work, this theoretical model is now checked by applying it to 2-methylpyrazine (2MP), which shows a different experimental behavior from that of pyridine.^[20]

Experimentally, SERS spectra of 2MP are characterized by two enhanced bands in the 1500–1600-cm⁻¹ region, which are assigned to the totally symmetric ring-stretching 8a,b modes. The 8a band is the strongest one at any electrode potential, whereas the weaker 8b band reaches the maximum enhancement at -0.50 V and afterward decreases at -0.75 V.

The SERS intensities of 2MP were already analyzed on the basis of the CT mechanism from the adsorbate point of view.^[22] Thus, the resonance process was established between the ground electronic state of the neutral molecule, S₀, and that corresponding to the radical anion named D₀ given that it is a doublet state. In that work,^[22] the minimum level of ab initio calculation, HF/3-21G, was employed, and the SERS-CT intensities were calculated by Peticolas' equation^[23] yielding only an explanation of the strong enhancement of the 8a band. In this work, the effect of the electrode potential in SERS intensities as well as in wavenumber shifts of 2MP is now analyzed by considering the whole metal-adsorbate supermolecule [Ag_n-2MP]^q and the two possible adsorption centers through the two non-equivalent nitrogen atoms. In addition, the SERS-CT intensities are now calculated by independent mode displaced harmonic oscillator (IMDHO) method,^[18,24] and the level of theoretical calculation is updated, employing time-dependent DFT (TD-DFT) methodology. In this way, a comparison between the predictive capabilities of both theoretical models, that is, the metal-adsorbate supermolecule or the isolated adsorbate, can be established. Moreover, the analysis of the data corresponding to the two types of complexes, [Ag_n-N1]^q and [Ag_n-N4]^q, would allow to identify its adsorption molecular center.

Thus, one of the goals of this work is to check the comparative performance of simple theoretical models, isolated adsorbate and supermolecule, in predicting SERS properties (wavenumbers/intensities) and to demonstrate that the second one together with DFT calculations improves the intensity results, explaining, for instance, the selective enhancement of the 8b mode in SERS of 2MP, a band that only shows strong intensity in particular molecules.

2 | MATERIALS AND METHODS

2.1 | Electronic structure calculation

The 2MP structure has been optimized at M06-HF/LanL2DZ^[25,26] level of calculation under a C_s symmetry. The most stable geometry shows a hydrogen atom of the methyl group located in the plane in trans-position with respect to the nearest nitrogen atom, although the

rotational barrier of the methyl group is small and amounts to only 0.2 Kcal/mol.

The electrode potential has been simulated by different linear silver atoms ($n = 2, 3$) with different charges ($q = 0$ for $n = 2$ and $q = \pm 1$ for $n = 3$) linked to each nitrogen atom of 2MP, yielding two types of surface complexes, [Ag_n-N1]^q and [Ag_n-N4]^q. A perpendicular orientation of adsorbate with respect to the metallic surface is then assumed. These metallic clusters account for the effect of a fractionary surface excess of charge of the electrode ($q_{\text{eff}} = q/n$) on the properties of the surface metal-molecule supermolecule. It has been previously demonstrated that this range of $\Delta q_{\text{eff}} \approx 0.66$ a.u. would correspond with the here discussed range of electrode potentials $\Delta V \approx 1$ V.^[19,20] The geometry of all surface complexes was optimized, and their respective excited electronic states were also investigated. The M06-HF functional^[25] with the LanL2DZ basis set^[26] (D95 basis set for the first-row atoms and the Los Alamos plus DZ effective core pseudopotential for the silver) has been selected to identify the CT electronic states in the different complexes and to calculate afterward the SERS-CT intensities. This level of calculation has been used in previous works what allows for comparing the results obtained for different adsorbates.^[16,20,21]

All DFT calculations were carried out with the GAUSSIAN16 program.^[27] The vibrational wavenumbers, molecular orbitals, and excited states have been analyzed with the help of the visualization MOLDEN program.^[28]

2.2 | Calculation of SERS-CT intensities

The IMDHO method^[24,29] has been used to calculate the SERS-CT intensities by assuming that the excited-state displacements with respect to the ground state geometry are proportional to the gradient (forces) calculated at the Franck–Condon point of the excited state potential energy surface. No normal mode rotation between both electronic states involved in the resonance process is considered.

According to this model, the intensity I_i of a Raman band of wavenumber ω under preresonance conditions with a particular excited state is proportional to the square of the respective dimensionless shift parameter of Manneback,^[30] Δ_i :

$$I_i \propto \Delta_i^2 \omega_i^2 \quad (1)$$

This shift parameter is calculated within the harmonic approximation^[29,31]:

$$\Delta_i \propto \omega_i^{-3/2} f M^{-1/2} L_i \quad (2)$$

where f is the gradient vector of the excited state evaluated at the Franck–Condon geometry, M is the diagonal matrix of atomic masses, and L_i is the eigenvector of the Hessian matrix associated with the i -normal mode.

This method has two advantages with respect to Petricolas' equation.^[23] First, it works in Cartesian coordinates instead of internal coordinates, and second, it is not necessary to optimize the geometry in the excited state, which usually is difficult to converge because of potential energy surface crossing.

3 | RESULTS AND DISCUSSION

3.1 | Main features of Raman and SERS spectra of 2MP

Raman and SERS spectra of 2MP were recorded elsewhere,^[22] and the vibrational assignment based on the RFH/3-21G ab-initio scaled force field methodology by Pulay et al.^[32] was also reported. The Raman spectrum is dominated by three strong bands recorded at about 830, 1032, and 1069 cm^{-1} and assigned to $1; \nu_{\text{ring}}$, $12; \delta_{\text{ring}}$, and δ (CH) normal modes, respectively, according to Wilson's nomenclature.^[33] However, all SERS spectra are very different from that of the normal Raman solution (Figure 1). The main characteristic of SERS is the selective enhancement of the band assigned to the totally symmetric 8a ring-stretching mode recorded at 1600 cm^{-1} , being the strongest band at any potential, even in the spectrum recorded at 0.00 V, unlike the SERS spectra of pyridine^[20] and 3-methylpyridine^[8] where SERS spectrum recorded at 0.00 V looks like similar to the aqueous solution Raman spectra. There is other enhanced band recorded at about 1520 cm^{-1} that is assigned to the totally symmetric 8b mode. This band reaches half the intensity of the 8a band at -0.50 V, and thereafter, it decreases at -0.75 V.

Regarding the shifts, Table S1, of the SERS wavenumbers with respect to those recorded in the Raman of the aqueous solution ($\Delta\nu_{\text{ads.,V}} = \nu_{\text{SERS,V}} - \nu_{\text{Raman}}$), there are two general trends caused by the adsorption on the charged electrode. The δ (CH), 12, and 6a,b modes are blue-shifted at positive voltages with respect to the zero-charge potential (-0.50 V), with shifts amounting to $\Delta\nu_{\text{ads.,0.0V}} = +4, +9, +11,$ and $+5 \text{ cm}^{-1}$ at 0.00 V, and $\Delta\nu_{\text{ads.,-0.25V}} = +2, +5, +9,$ and $+5 \text{ cm}^{-1}$ at -0.25 V, respectively, being red-shifted at more negative voltages ($\Delta\nu_{\text{ads.,-0.75V}} = -5, -4, -1,$ and -1 cm^{-1} at -0.75 V). However, both 8a,b modes show red-shifts in all the

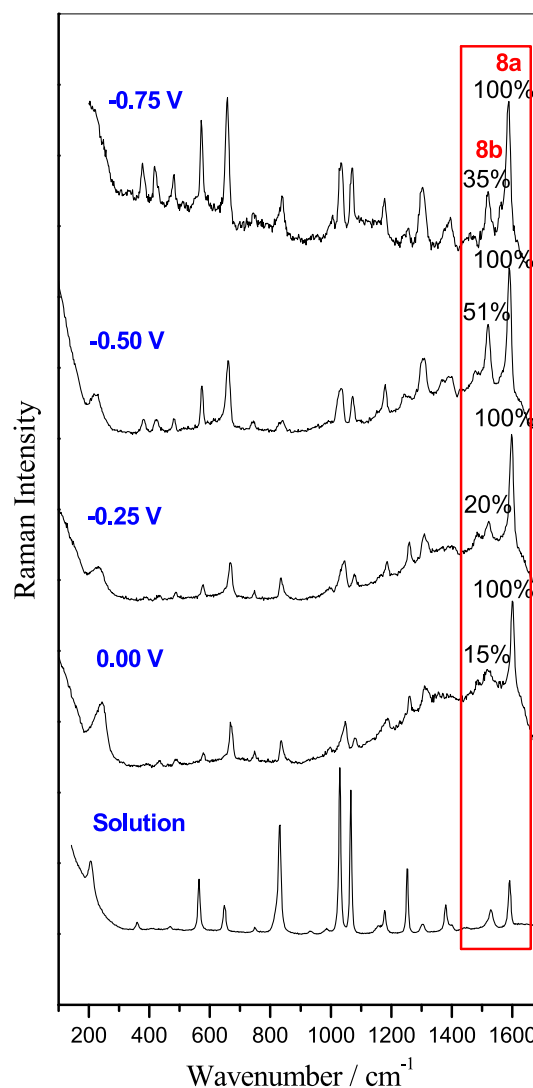


FIGURE 1 Raman spectrum of 1M aqueous solution of 2MP and SERS spectra of 2MP/KCl (0.1M/0.1M) solutions recorded on nanostructured silver surface at different electrode potentials using 514.5-nm excitation line [Colour figure can be viewed at wileyonlinelibrary.com]

voltage range, 8b mode exhibiting a significant shift of $\Delta\nu_{\text{ads.,-0.25V}} = -21 \text{ cm}^{-1}$ at -0.25 V. Only 8a, 12, and 6a modes undergo significant red-shifts with amplitudes, ($\Delta\nu_{\text{v,exp}} = \Delta\nu_{\text{ads.,-0.75V}} - \Delta\nu_{\text{ads.,0.0V}}$), of about -10 cm^{-1} summarized in the first column of Table 1, in a similar way that it happens in SERS spectra of pyridine.^[20]

3.2 | Wavenumber shifts due to the adsorption on a charged silver surface at different electrode potentials

M06-HF/LanL2DZ wavenumber shifts ($\Delta\nu_{[\text{Agn-N}]^q} = \nu_{[\text{Agn-N}]^q} - \nu_{2\text{MP}}$) of the most representative totally

symmetric normal modes corresponding to the two $[\text{Ag}_n\text{-2MP}]^q$ complexes are collected in Table 1.

Although DFT calculations predict that all N1 complexes are slightly more stable (<1 Kcal/mol) than N4 in any selected cluster, they do not reproduce the experimental behavior of the most characteristics 8a,b modes. For instance, they predict a blue-shift of $\Delta\nu_{[\text{Ag}_2\text{-N1}]^0} = +6$ cm^{-1} for the 8a mode in the $[\text{Ag}_2\text{-N1}]^0$ system. However, red-shifts are calculated for the two 8a,b vibrational modes in the case of the N4 complex, $[\text{Ag}_2\text{-N4}]^0$, with $\Delta\nu_{[\text{Ag}_2\text{-N4}]^0} = -2$ and -12 cm^{-1} , respectively, in agreement with the experimental results ($\Delta\nu_{\text{ads},0.0\text{V}} = -3$ and -22 cm^{-1} for 8a,b, respectively).

Although the calculated M06-HF/LanL2DZ energy barrier of the methyl group is very small, about 0.80 and 0.21 Kcal/mol in $[\text{Ag}_2\text{-N1}]^0$ and $[\text{Ag}_2\text{-N4}]^0$ complexes respectively, the calculated wavenumbers of 2MP bonded to silver can be dependent on the rotation of the methyl group, especially in N1 complexes due to the proximity of the methyl to the metallic surface. The wavenumbers of 8a,b modes in the complexes with the methyl hydrogen atom in *cis*-position with respect to the aromatic nitrogen were also calculated and collected in Table 1 (shown in parenthesis). The wavenumbers of the *cis*-N4 complex do not undergo significant changes, whereas those of the N1 complex seem to be slightly affected by the proximity of the methyl group to the silver atoms. The calculations estimated a red-shift in the case of neutral *cis*-N1 complex, $\Delta\nu_{[\text{Ag}_2\text{-N1}]^0} = -10$ and -13 cm^{-1} for 8a,b modes, respectively, in agreement with SERS recorded at

-0.50 V ($\Delta\nu_{\text{ads},-0.50\text{V}} = -12$ and -19 cm^{-1}). This voltage is close to the potential of zero charge of a polycrystalline silver electrode,^[34,35] and thus, it correlates well with the results obtained for the $[\text{Ag}_2\text{-2MP}]^0$ complex.

The effect of applying negative potentials is, generally speaking, to shift the SERS wavenumbers toward the red, being the amplitude ($\Delta\nu_{\text{v,exp}}$) corresponding to 8a, 12, and 6a modes of approximately 10 cm^{-1} , in a similar way that it happens in SERS of pyridine.^[20] The theoretical values ($\Delta\nu_{\text{v,calc}}$) for both N1 and N4 complexes reproduce the experimental behavior in almost every normal modes. This means that there exists a good correlation between the experimental (V, macroscopic applied bias in electrochemical experiments) and theoretical ($q_{\text{eff}} = q/n$, microscopic density of charge of the metal surface) parameters, which modulates the wavenumbers and relative intensities of the recorded and calculated SERS spectra, respectively. There is only a discrepancy between the calculated values for the two types of complexes in the case of 6b and 1 modes, whereas in the N1 complex, it is predicted a blue- and red-shift, respectively, in the entire voltage range, yielding an amplitude of $\Delta\nu_{\text{v,calc}} = -8$ and $+9$ cm^{-1} in agreement with the experiment ($\Delta\nu_{\text{v,exp}} = -6$ and $+6$ cm^{-1} for 6b and 1 modes), a red- and blue-shift ($\Delta\nu_{[\text{Ag}_n\text{-N4}]} = -2, 0, +3$ cm^{-1} for 6b mode and $\Delta\nu_{[\text{Ag}_n\text{-N4}]} = +11, +4, +4$ cm^{-1} for 1 mode) is calculated for the three studied theoretical complexes of the N4 system, with an amplitude of $\Delta\nu_{\text{v,calc}} = +5$ and -7 cm^{-1} , which does not reproduce the observed result.

TABLE 1 Experimental and calculated (M06-HF/LanL2DZ) wavenumber shifts and amplitudes (cm^{-1}) for selected totally symmetric normal modes of 2MP due to surface adsorption

Mode	$\Delta\nu_{\text{v,exp}}^a$	M06-HF/LanL2DZ Adsorption shifts ^b			$\Delta\nu_{\text{v,calc}}^d$	M06-HF/LanL2DZ Adsorption shifts ^b			$\Delta\nu_{\text{v,calc}}^d$
		$\Delta\nu$	$\Delta\nu$	$\Delta\nu$		$\Delta\nu$	$\Delta\nu$	$\Delta\nu$	
		$[\text{Ag}_3\text{-N1}]^+$	$[\text{Ag}_2\text{-N1}]^0$	$[\text{Ag}_3\text{-N1}]^-$		$[\text{Ag}_3\text{-N4}]^+$	$[\text{Ag}_2\text{-N4}]^0$	$[\text{Ag}_3\text{-N4}]^-$	
8a; ν_{ring}	-11	+8 (-15) ^c	+6 (-10) ^c	+5 (-10) ^c	-3	+10 (+9) ^c	-2 (+1) ^c	+6 (+5) ^c	-4
8b; ν_{ring}	+3	-3 (-13) ^c	-4 (-13) ^c	-3 (-12) ^c	0	0 (-2) ^c	-12 (-11) ^c	0 (-2) ^c	0
$\nu(\text{CX})$	-1	+3	-2	+5	+2	+7	+1	+4	-3
$\delta(\text{CH})$	-9	+11	+3	+2	-9	+17	0	+7	-10
12; δ_{ring}	-13	+19	+11	+3	-16	+6	+1	0	-6
1; ν_{ring}	+6	-9	-7	0	+9	+11	+4	+4	-7
6a; δ_{ring}	-12	+13	+7	+4	-9	+24	+16	+15	-9
6b; δ_{ring}	-6	+10	+5	+2	-8	-2	0	+3	+5

$$^a \Delta\nu_{\text{v,exp}} = \Delta\nu_{\text{ads},-0.75\text{V}} - \Delta\nu_{\text{ads},0.0\text{V}}$$

$$^b \Delta\nu_{[\text{Ag}_n\text{-N}]^q} = \nu_{[\text{Ag}_n\text{-N}]^q} - \nu_{2\text{MP}}$$

^cShift between the wavenumbers calculated for the two $[\text{Ag}_2\text{-Nx}]$ complex with a hydrogen atom of the methyl group in *cis*-position with respect to nearest aromatic nitrogen atom.

$$^d \Delta\nu_{\text{v,calc}} = \nu_{[\text{Ag}_3\text{-N}]^-} - \nu_{[\text{Ag}_3\text{-N}]^+}$$

3.3 | SERS-CT intensities. Theoretical predictions from isolated adsorbate and metal-adsorbate supermolecule models

Figure S1 shows the calculated M06HF/LanL2DZ SERS-CT spectrum compared with previously published at HF/3-21G* level^[22] by assuming that the S_0 - D_0 transition of isolated adsorbate corresponds to the CT process. Both calculations predict the selective enhancement of the 8a band. This result agrees roughly with the relative intensities of the spectrum recorded at 0.0 V and confirms the presence of a resonant metal-to-molecule electron transfer in SERS, but this approach cannot explain the enhancement of the 8b band, for instance, in the SERS recorded at negative electrode potential as it occurs in the case of 3MPy.^[8] Thus, no level of calculations, ab initio and DFT, applied to the isolated adsorbate model are able to reproduce the experimental data. In addition, these calculations do not allow to distinguish between the two types of complexes bonded to silver through N1 or N4 nitrogen atoms.

However, the use of a metal-adsorbate supermolecule model together with DFT calculations allows to improve the theoretical results, and it can predict the enhancement of the 8b mode. In this way, a comparison between ab initio and DFT results is investigated for the neutral $[\text{Ag}_2\text{-2MP}]^0$ complex with the aim to establish which type of calculation works better. Electronic structure calculations of singlet excited states of the neutral $[\text{Ag}_2\text{-2MP}]^0$ complex were carried out at two levels, by using ab initio configuration interaction single (CIS)^[36] approach and time-dependent M06-HF^[25] calculations with the LanL2DZ basis set in both cases. Tables S2 and S3 collect the main properties of the excited electronic states calculated at the Franck-Condon point. Two CT states can be identified below 5 eV in both complexes (Table S2). The first CT_0 state (HOMO;Ag-to-LUMO;2MP) is calculated at 3.97 and 4.07 eV for N4 and N1 complexes given that they are characterized by a transferred charge (Δq) from the metal to the molecule of $\Delta q = 0.79$ and 0.67 a.u., respectively. The geometry optimization of these CT states yields lower energies of 3.49 and 3.58 eV for N4 and N1 complexes, respectively. Taking into account that the calculated CIS/LanL2DZ energies are overestimated about 25%,^[8] resonance or preresonance up to these CT states can be established under green laser excitation (2.5 eV at 514.5 nm). Other CT state is calculated at higher energy (HOMO;Ag-to-LUMO+1;2MP), 4.96 and 5.03 eV, with $\Delta q = 0.86$ and 0.53 a.u. for the N4 and N1 complexes, respectively. The optimized energy of these states is 4.48 and 4.53 eV, respectively, being the energy difference between the pair of CT states about 1 eV in both complexes.

Figure 2a shows the calculated CIS/LanL2DZ spectra of N1 and N4 complexes for the respective S_0 - CT_0 resonance transitions. In both spectra, the strongest enhancement is shown by vibration 8a as occurred in the previous calculations considering the S_0 - D_0 resonance of isolated adsorbate Figure S1. In the case of the N1 complex, it is also predicted a rather weak enhancement of the 8b band, in agreement with the SERS at 0.0 V.

These results are improved by using TD-M06-HF calculations (Figure 2b). The first CT_0 excited state of the N4 and N1 neutral complexes is calculated at 2.93 and 2.87 eV, with transferred charges of 0.69 and 0.57 a.u., respectively (Table S3). SERS-CT spectra calculated for the S_0 - CT_0 transition now predict the enhancement of the two 8a,b bands with relative intensities of 100 and about 50–70 for the two complexes, respectively, in agreement with the experimental behavior of the SERS recorded at -0.50 or -0.75 V. The calculated intensity corresponding to the 8b mode diminishes about 20% by considering the cis-conformation of the methyl group with respect to the closest nitrogen.

Therefore, the DFT electronic structure of the neutral $[\text{Ag}_2\text{-2MP}]^0$ complex account for the differentiated activity of vibrations 8a,b in SERS. The observed enhancement of the 8a and 8b bands is due to Franck-Condon factors (A-term), as happens in other aromatic molecules with low symmetry like 3-methylpyridine,^[8] or even in systems where the operating symmetry is reduced by the adsorption on the metal, as it occurs in the case of pyrimidine.^[37] Herzberg-Teller contributions (B-term in RR) do not seem to play an important role in SERS of 2MP.

3.4 | Dependence of the SERS-CT intensities of 8a,b modes on the electrode potential

Tables S4 and S5 summarize the TD-M06-HF/LanL2DZ calculated results of the excited singlets of charged $[\text{Ag}_3\text{-2MP}]^+$ and $[\text{Ag}_3\text{-2MP}]^-$ complexes, respectively. Figure 3 shows the theoretical SERS-CT spectra for the neutral $[\text{Ag}_2\text{-N1,N4}]^0$ and charged $[\text{Ag}_n\text{-N1,N4}]^q$ complexes and the experimental SERS spectra recorded at different electrode potentials. Both types of coordination reproduce the experimental dependence of the intensities of the 8a,b bands on the applied voltage. 8a mode is the strongest band in all calculations in agreement with the experiments. However, the weak 8b band recorded at 0.00 V becomes stronger in the SERS at -0.50 V and thereafter diminishes its intensity at -0.75 V. This is just the behavior shown by the calculated SERS-CT spectra for both $[\text{Ag}_n\text{-N1}]^q$ and $[\text{Ag}_n\text{-N4}]^q$ series of complexes.

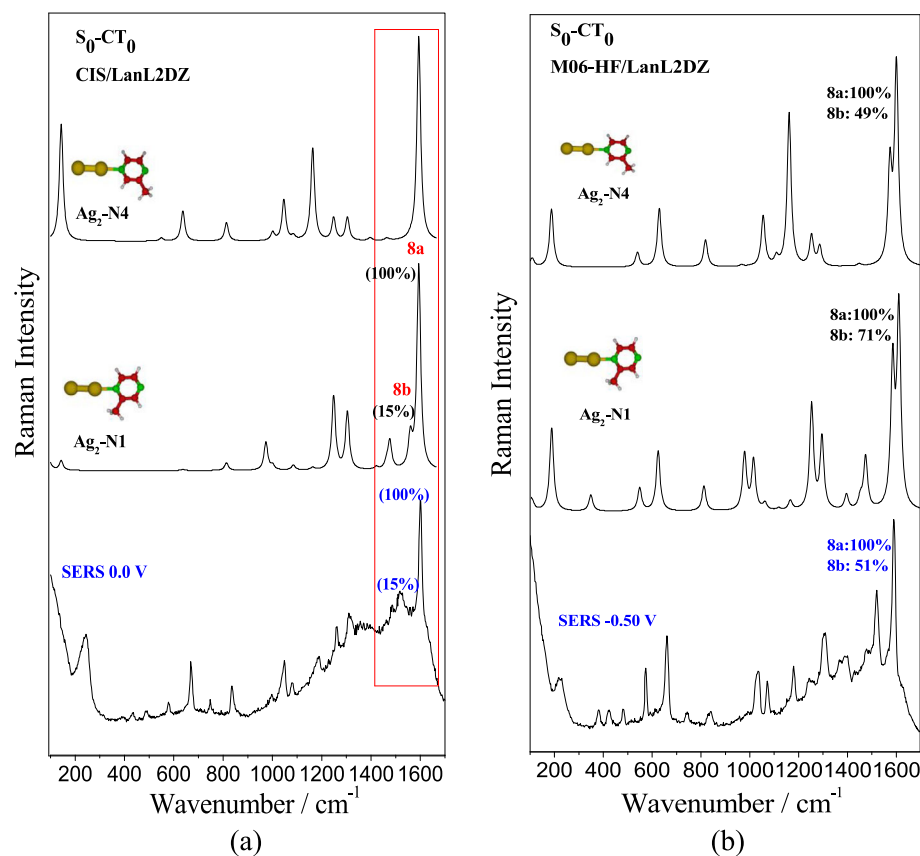


FIGURE 2 Calculated SERS-CT spectra involving the S_0 -CT $_0$ transition for the two $[Ag_2-2MP]^0$ N1 and N4 complexes at (a) CIS/LanL2DZ level and (b) M06-HF/LanL2DZ level of calculations compared to the SERS recorded at 0.00 and -0.50 V [Colour figure can be viewed at wileyonlinelibrary.com]

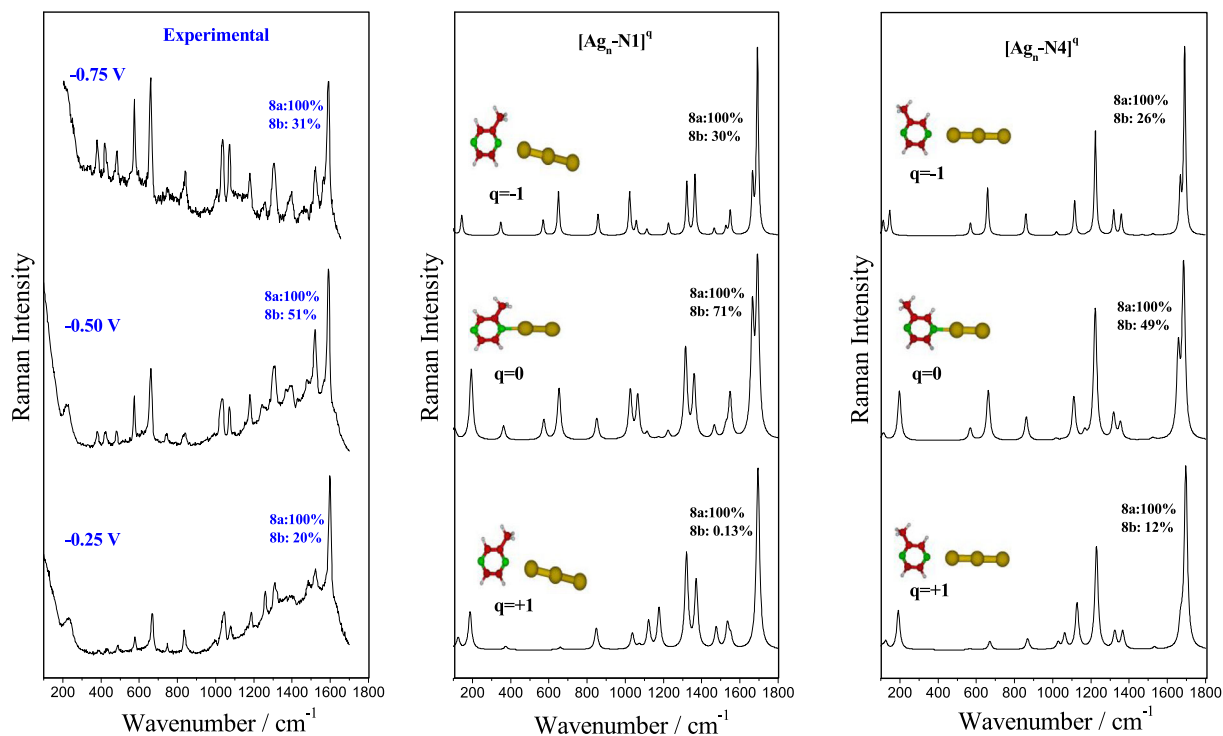


FIGURE 3 Electrochemical SERS spectra of 2MP (left) and calculated M06-HF/LanL2DZ SERS-CT spectra involving the S_0 -CT $_0$ transition of $[Ag_n-N1]^q$ complexes (middle) and $[Ag_n-N4]^q$ complexes (right) [Colour figure can be viewed at wileyonlinelibrary.com]

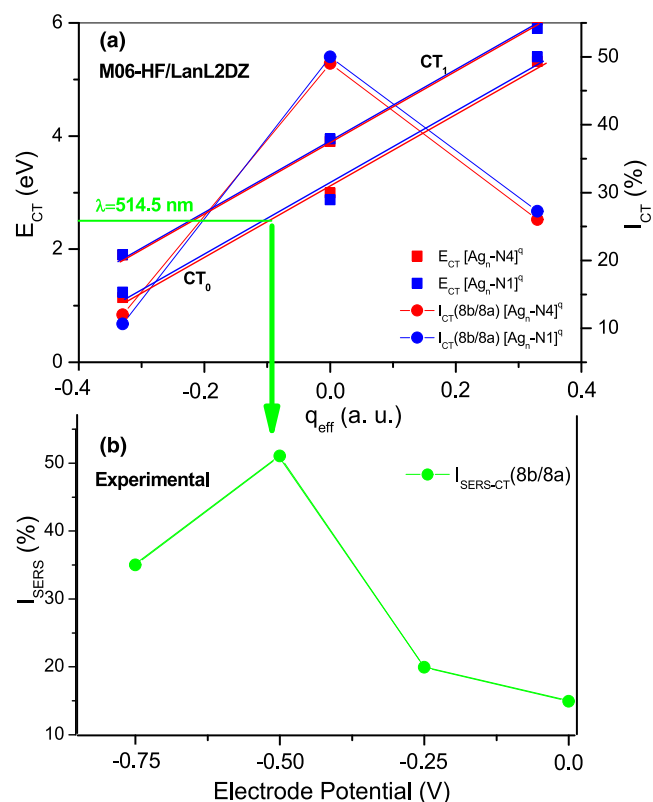


FIGURE 4 (a) M06-HF/LanL2DZ energies of the $CT_{0,1}$ states (square) and calculated ratio (circle) between the intensities of the 8b/8a vibrations for $[Ag_n-N1]^q$ (blue) and $[Ag_n-N4]^q$ (red) complexes. (b) Experimental dependence of the SERS intensity ratio of 8b/8a modes on the electrode potential [Colour figure can be viewed at wileyonlinelibrary.com]

The characteristic SERS-CT bands corresponding to 8a and 8b modes are much weaker in the SERS recorded at -0.75 V. This can be due to the energy of the CT state becoming out of resonance as the electrode potential is made more negative. The energy of the CT levels is tuned by the potential, and therefore, the calculated energies are very sensitive to the charge density of the metal cluster (q_{eff}) as can be seen in Tables S3–S5.

There is a linear dependence between the energy of the CT states and the effective charge of the metal clusters (q_{eff}) as can be seen in Figure 4a. The respective slopes quantify the effectiveness of q_{eff} in tuning the energy of the CT state, that is, the dependence of the metal-to-molecule CT process on the applied electrode potential. Slopes amount to 6.33 and 6.30 eV/a.u. for the CT_0 state of the N4 and N1 complexes, respectively. These values are very similar to that obtained in the cases of Rh- or Ag-pyridine complexes, 6.35 and 6.69 eV/a.u., respectively.^[19] The effectiveness of q_{eff} in tuning the CT state and its relative position with respect to the energy of the 514.5 nm exciting line (2.5 eV) can be also seen in

Figure 4. This figure also shows the dependence of the calculated (Figure 4a) and observed (Figure 4b) ratio between the intensities of the 8a and 8b modes on q_{eff} and the electrode potential, respectively.

TD-M06-HF energies of the CT states of neutral $[Ag_2-2MP]^0$ complexes (2.99 and 2.87 eV, for $[Ag_2-N4]^0$ and $[Ag_2-N1]^0$, respectively) are in the order of the incident photon. Therefore, it can be concluded that the $[Ag_2-2MP]^0$ complex would correspond to the experimental reached at -0.50 V, whereas the positive and negative $[Ag_3-2MP]^q$ complexes would correspond to the SERS recorded at -0.25 and -0.75 V, respectively. This correlation allows relating the theoretical q_{eff} parameter to the experimental values of electrode potentials as it was carried out in other systems like Rh-pyridine and Rh-adenine.^[19]

4 | CONCLUSION

Electrochemical SERS spectra of 2MP are dominated by a metal-to-molecule CT mechanism in the studied electrode potential range. The CT resonance condition is reached under 514.5-nm excitation line at -0.50 V. Under these experimental conditions, it is observed the selective enhancement of the bands assigned to 8a,b normal modes, being the 8a band the strongest one at any potential. A simple theoretical model based on a linear silver cluster with different charge densities was used with the aim to simulate the effect of the electrode potential on the properties of the metal-adsorbate supermolecule in the ground and CT excited electronic states. RR intensities calculated from closed-shell TD-DFT calculations performed for the two types of complexes $[Ag_n-N1]^q$ and $[Ag_n-N4]^q$ reproduce the dependence of the selective and relative enhancement of the intensities of the 8a,b modes on the applied voltage. Both types of complexes are also able to reproduce the shifts of the wavenumbers of the main SERS bands. In addition, there are no significant differences between the predictions derived from the two types of complexes regarding the relative intensities. Therefore, it is not possible to derive which aromatic nitrogen, N1 or N4, is involved in the adsorption process on the basis of theoretical calculations.

ACKNOWLEDGEMENTS


This research has been supported by Junta de Andalucía/FEDER (UMA18-FEDERJA-049 and P18-RT-4592). D.A. acknowledges the University of Málaga and Generalitat Valenciana/European Social Fund (APOSTD/2021/025) for postdoctoral contracts. The authors thanks to the Supercomputing and Bioinnovation Center (University of Málaga) for computational

resources and Rafael Larrosa for technical support. Funding for open access: Universidad de Málaga/CBUA.

DATA AVAILABILITY STATEMENT


Subscription article; Data openly available in a public repository that issues datasets with DOIs.

ORCID

Samuel Valdivia  <https://orcid.org/0000-0002-2752-976X>

Daniel Aranda  <https://orcid.org/0000-0003-0747-6266>

Juan Soto  <https://orcid.org/0000-0001-6702-2878>

Juan Carlos Otero  <https://orcid.org/0000-0003-4078-6258>

Isabel López-Tocón  <https://orcid.org/0000-0003-2351-1543>

REFERENCES

- [1] R. Aroca, *Surface-enhanced Raman vibrational spectroscopy*, John Wiley & Sons, Chichester **2006**.
- [2] E. Le Ru, P. Etchegoin, *Principles of surface-enhanced Raman spectroscopy: And related Plasmonic effects*, Elsevier, Amsterdam, The Netherlands **2008**.
- [3] J. A. Creighton, *Surf. Sci.* **1986**, *173*, 665.
- [4] I. López-Tocón, E. Imbarack, J. Soto, S. Sanchez-Cortes, P. Leyton, J. C. Otero, *Molecules* **2019**, *24*, 4622.
- [5] J. Soto, E. Imbarack, I. López-Tocón, S. Sanchez-Cortes, J. C. Otero, P. Leyton, *RSC Adv.* **2019**, *9*, 14511.
- [6] J. A. Creighton, in *The selection rules for surface-enhanced Raman spectroscopy. In spectroscopy of surfaces*, (Eds: R. H. J. Clark, R. E. Hester), Wiley, New York **1988** 37.
- [7] J. Roman-Perez, I. Lopez-Tocon, J. L. Castro, J. F. Arenas, J. Soto, J. C. Otero, *Phys. Chem. Chem. Phys.* **2015**, *17*, 2326.
- [8] S. P. Centeno, I. López-Tocón, J. Roman-Perez, J. F. Arenas, J. Soto, J. C. Otero, *J. Phys. Chem. C* **2012**, *116*, 23639.
- [9] S. Valdivia, D. Aranda, F. J. Ávila Ferrer, J. Soto, I. López-Tocón, J. C. Otero, *J. Phys. Chem. C* **2020**, *124*(32), 17632.
- [10] W.-H. Yang, G. C. Schatz, *J. Chem Phys.* **1992**, *97*(5), 3831.
- [11] M. Moskovits, D. P. DiLella, K. J. Maynard, *Langmuir* **1988**, *4*, 67.
- [12] A. Otto, J. Billmann, J. Eickmans, U. E. C. Pettenkofer, *Surf. Sci.* **1984**, *138*(2-3), 319.
- [13] J. R. Lombardi, R. L. Birke, T. Lu, J. Xu, *J. Chem. Phys.* **1986**, *84*, 4174.
- [14] D. Aranda, S. Valdivia, F. J. Avila, J. Soto, J. C. Otero, I. Lopez-Tocon, *Phys. Chem. Chem. Phys.* **2018**, *20*, 29430.
- [15] M. Sardo, C. Ruano, J. L. Castro, I. López-Tocón, J. Soto, P. Ribeiro-Claro, J. C. Otero, *Phys. Chem. Chem. Phys.* **2009**, *11*, 7437.
- [16] F. Avila, C. Ruano, I. Lopez-Tocon, J. F. Arenas, J. Soto, J. C. Otero, *Chem. Commun.* **2011**, *47*, 4213.
- [17] W. E. Doering, S. Nie, *J. Phys. Chem. B* **2002**, *106*, 311.
- [18] R. J. H. Clark, T. J. Dines, *Angew. Chem., Int. Ed.* **1986**, *25*(2), 131.
- [19] J. Román-Pérez, C. Ruano, S. P. Centeno, I. López-Tocón, J. F. Arenas, J. Soto, J. C. Otero, *J. Phys. Chem. C* **2014**, *118*, 2718.
- [20] D. Aranda, S. Valdivia, J. Soto, I. Lopez-Tocon, F. J. Avila, J. C. Otero, *Front. Chem.* **2019**, *7*, 423.
- [21] S. Valdivia, J. F. Avila, J. C. Otero, I. López-Tocón, *Appl. Surf. Sci.* **2022**, *579*, 152071.
- [22] J. F. Arenas, I. L. Tocon, J. C. Otero, J. I. Marcos, *Vibr. Spectrosc.* **1999**, *19*(2), 213.
- [23] W. L. Peticolas, D. P. Strommen, V. Lakshminarayanan, *J. Chem. Phys.* **1980**, *73*, 4185.
- [24] A. C. Albretch, *J. Chem. Phys.* **1961**, *34*(5), 1476.
- [25] Y. Zhao, D. G. Truhlar, *J. Phys. Chem.* **2006**, *110*, 5121.
- [26] P. J. Hay, W. R. Wadt, *J. Chem. Phys.* **1985**, *82*, 270.
- [27] Gaussian 16, *Revision, a.03*, Gaussian, Inc, Wallingford, CT, USA **2016**.
- [28] G. Schaftenaar, J. H. Noordik, *J. Comput.-Aided Mol. Des.* **2000**, *14*, 123.
- [29] D. A. Long, *The Raman effect: A unified treatment of the theory of Raman scattering by molecules*, John Wiley & Sons, Ltd, West Sussex England, UK **2002**.
- [30] C. Manneback, *Physica* **1951**, *17*, 1001.
- [31] D. Aranda, F. J. Avila, I. López-Tocón, J. F. Arenas, J. C. Otero, J. Soto, *Phys. Chem. Chem. Phys.* **2018**, *20*, 7764.
- [32] P. Pulay, G. Fogarasi, J. E. Boggs, *J. Chem. Phys.* **1981**, *74*, 3999.
- [33] G. Varsanyi, *Vibrational spectra of benzene derivatives*, Academic Press, Cambridge, MA, USA **1969**.
- [34] X. Y. Chen, A. Otto, *J. Raman Spectrosc.* **2005**, *36*(6-7), 736.
- [35] J. T. Hupp, D. Larkin, M. J. Weaver, *Surf. Sci.* **1983**, *125*, 429.
- [36] J. B. Foresman, M. Head-Gordon, J. A. Pople, M. J. Frisch, *J. Phys. Chem.* **1992**, *96*(1), 135.
- [37] S. P. Centeno, I. López-Tocón, J. F. Arenas, J. Soto, J. C. Otero, *J. Phys. Chem. B* **2006**, *110*, 14916.

SUPPORTING INFORMATION

Additional supporting information can be found online in the Supporting Information section at the end of this article.

How to cite this article: S. Valdivia, D. Aranda, J. Soto, J. C. Otero, I. López-Tocón, *J Raman Spectrosc* **2023**, *54*(2), 150. <https://doi.org/10.1002/jrs.6475>